Journal of Fluorescence (2019) 29:271–277
https://doi.org/10.1007/s10895-018-02337-1

ORIGINAL ARTICLE

Selective Sensing of Iron by Pyrrolo[2,3-*c*]Quinolines

Togiti Uday Kumar[1] · Shweta Pawar[1] · Amit Nag[1] · Anupam Bhattacharya[1]

Received: 14 September 2018 / Accepted: 26 December 2018 / Published online: 8 January 2019

Abstract

This paper reports development of an iron sensor, 2-(3*H*-pyrrolo[2,3-*c*]quinolin-4-yl)aniline (APQ). The fluorophore facilitates micromolar detection of Fe^{3+}/Fe^{2+} in the presence of various cations, including well-known interfering cations $Co^{2+}$and Cu^{2+} by the process of fluorescence quenching.

Keywords Pyrrolo-quinoline · Iron sensing · ESIPT · Quenching · Logic gate

Introduction

Iron in both its +2 and + 3 oxidation state is one of the most important transition metal in living systems. It serves as a cofactor in diverse biochemical reactions/processes such as oxidoreductase catalysis, oxygen transport and electron transport. Both excess and deficiency of this metal is known to induce wide spectrum of diseases ranging from liver cancer, liver cirrhosis, anaemia to Parkinson's disease, arthritis, diabetes, malaria and even heart failure [1–4]. Thus, selective sensing of iron is of considerable importance to human health. Various techniques such as atomic absorption spectroscopy [5], spectrophotometry [6–8], voltammetry [9–11] and chemiluminescence [12, 13], have been used for selective detection of iron. Some of these techniques, requiring sophisticated instrumentation along with elaborate pretreatment procedures are inappropriate for in-field or on-line monitoring. While potentiometric sensors offer advantages owing to their simple, rapid and non-destructive characteristics, they are plagued by the problem of low response slopes due to a charge of analyzed ions. All these concerns are effectively addressed by colorimetric and fluorescence techniques, which allow sub-ppm level detection along with the possibility of intracellular monitoring. Additionally, fluorescence sensors are also bestowed with features like fast response time and technical simplicity. These advantages have catapulted the fluorescence based analytical techniques at the forefront of selective iron sensing [14, 15].

In a recent report by Lan et al., oligothiophenes were used for selective iron sensing in aqueous condition [16]. Coumarin based fluorophores were used by Hua et al. and Zhao et al. for selective turn-OFF fluorescent sensing of Fe^{3+} in DMSO and in aqueous medium, respectively [17, 18]. In a separate work, Pant and coworkers reported coumarin-triazole compounds for selective iron sensing using turn-OFF fluorescence technique [19]. A chemosensor derived from vitamin B_6 cofactor pyridoxyl-5-phosphate was used by Sharma et al., for selective detection of iron in aqueous medium [20]. 5-hydroxybenzo[g]indoles were used by Pramanik and coworkers for selective turn-OFF iron sensing [21]. Iron sensors using fluorescence signaling process can be classified into three types: turn-ON [16, 22, 23], turn-OFF [17–21, 24], and ratiometric [25–27], with significant share garnered by fluorescence turn-OFF techniques. Main reason for such behaviour is generally attributed to Fe^{3+} assisted photoinduced electron transfer and/or exited state de-excitation pathways (via electronic energy transfer) [15].

We have an ongoing interest in the area of ion sensing. Towards this effort, we have looked at selective Zn^{2+} and F^- sensing by using easy to assemble 4-substituted pyrrolo[2,3-*c*]quinolines as fluorophores [28, 29]. The work reported in this communication attempts to expand the scope of these compounds to selective sensing of Fe^{3+}.

Electronic supplementary material The online version of this article (https://doi.org/10.1007/s10895-018-02337-1) contains supplementary material, which is available to authorized users.

✉ Anupam Bhattacharya
anupam@hyderabad.bits-pilani.ac.in

[1] Department of Chemistry, Birla Institute of Technology and Science-Pilani, Hyderabad Campus, Hyderabad 500078, India

Results and Discussion

Given the general tendency of fluorescence based iron detection via quenching pathway and the simplicity of fluorophore requirements, we decided to design fluorophores for these study with ligands **1** and **2** reported by Ghosh et al. and Zhang et al. (Scheme 1) [24, 30]. Additional inputs for fluorophore design also came from several literature reports on quinoline based molecules [31–34]. Our familiarity with pyrrolo[2,3-*c*]quinoline systems prompted us to initiate this study with ligands APQ and HPQ bearing *o*-aniline and *o*-phenol as substituents. It was felt that presence of amino and hydroxyl functionality along with pyrrole nitrogen will provide suitable binding sites to the metal. Molecule HPQ has been already reported by us as a selective fluoride sensor [29].

Synthesis of the ligands was carried out by using modified Pictet-Spengler reaction as a key step [35]. The compounds were thoroughly characterized prior to UV-visible and fluorescence studies. Our approach was to look at steady state fluorescence behaviour of APQ and HPQ, individually, in DMF as a solvent and then carryout the same study by incubating the ligands with Fe^{3+} ion. Initial fluorescence screening revealed that while APQ exhibits an intensive fluorescence emission and a large Stokes shift of 115 nm, due to ESIPT reactions, it was subdued for HPQ with a comparatively low (67 nm) Stokes shift. Both the ligands displayed fluorescence quenching behaviour with Fe^{3+}, though the relative fluorescence decrease was less for HPQ in comparison with APQ. These primary results encouraged us to use APQ for further studies. Subsequently, fluorescence behaviour of APQ was examined by incubation with metals such as Ag^{+}, Ca^{2+}, Cd^{2+}, Co^{2+}, Cu^{2+}, Fe^{2+}, Hg^{2+}, K^{+}, Mg^{2+}, Na^{+}, Ni^{2+}, Pb^{2+}, Sn^{2+} and Zn^{2+} (Figs. 1 and 2). Modest increase in fluorescence intensity was noticed in case of most of the metals except Ni^{2+}, Sn^{2+} and Cu^{2+}, whereas Fe^{2+} also displayed fluorescence quenching.

To establish the selectivity of the molecule APQ towards Fe^{3+}, competitive fluorescence sensing experiments were also performed in the presence of other metals (Fig. 2). The observations clearly show that APQ is highly selective towards the detection of Fe^{3+} in presence of most of the other metals. It is noteworthy to mention here that APQ shows prominent selectivity towards Fe^{3+}, even in presence of well-known interfering cations $Co^{2+}$and Cu^{2+} [30].

With these initial results we explored binding stoichiometry between metal and ligand. It showed ratio of metal to ligand as 2:1. Association constant of the complex and detection limit were subsequently determined as 10×10^{6} M^{-2} and 0.4×10^{-6} M, respectively, using well established literature reports [36, 37]. Stoichiometry of the complex was also confirmed by the MALDI analysis, which showed a prominent peak at m/z 515.325 [$(M + Li^{+}$; $C_{17}H_{11}Cl_4Fe_2LiN_3^{+}$), exact mass m/z 515.856), thus establishing 2:1, metal to ligand ratio.

Further efforts were focused on probing the role played by pyrrole ring nitrogen in APQ. The main approach here was to introduce minor structural changes in the APQ structure and then examine its effect on Fe^{3+}/Fe^{2+} sensing. Accordingly, compounds 2-(3-methyl-3*H*-pyrrolo[2,3-*c*]quinolin-4-yl)aniline **(3)**, 2-(thieno[2,3-c]quinolin-4-yl)aniline **(4)** and 2-(4-phenylquinolin-2-yl)aniline **(5)** were synthesized (Fig. 3) [35, 38, 39]. Each of these molecules while retaining the basic quinoline core had pyrrole ring either modified or completely replaced. On screening these compounds with Fe^{3+} in DMF, fluorescence quenching was observed in all the cases. It was comparable to APQ in ligands **3** and **4** bearing *N*-methyl pyrrole and thiophene ring, respectively. Whereas, relative fluorescence intensity as well as fluorescence quenching was very less for ligand **5**. Thus, these results indicated that presence of pyrrole ring is not an absolute requirement for the selective sensing of Fe^{3+} ion.

We also carried out minor modification of aniline half of APQ scaffold by replacing benzene with pyridine ring while retaining the relative position of amino functionality

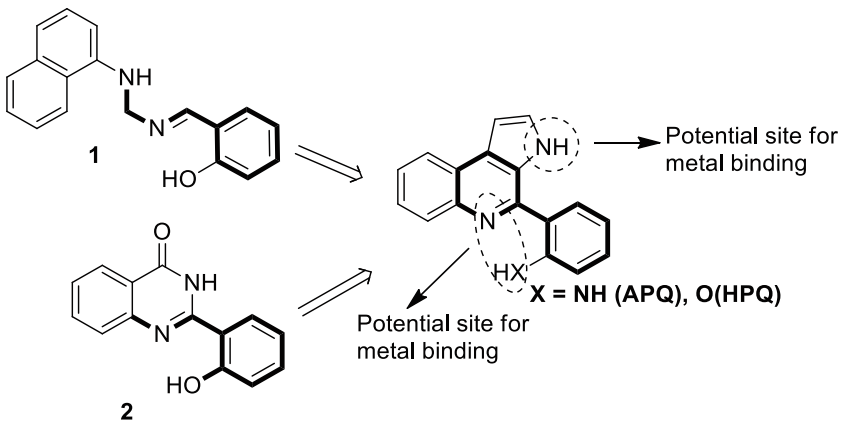

Scheme 1 Design of APQ and HPQ based on known ligands **1** and **2**

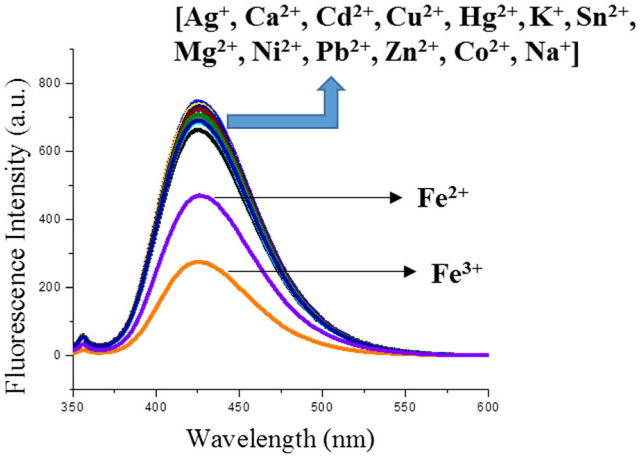

Fig. 1 Fluorescence behaviour of APQ on incubation with various metals

with respect to quinoline nitrogen **(6)** (Fig. 3) [35]. It also exhibited fluorescence quenching behaviour as APQ, on incubation with Fe^{3+} and Fe^{2+}, showing criticality of the amino functionality.

Subsequently, the reversibility of Fe^{3+} binding to APQ was tested by titration with EDTA, a well- known chelator for Fe^{3+}. While gradual enhancement of fluorescence signal on titration of Fe^{3+}-APQ complex with EDTA solution was noticed, it did not recover fully, which is clearly indicative of the high association constant of Fe^{3+}-APQ complex. The signal was again quenched on further addition of Fe^{3+} solution. This experiment helped us to establish a somewhat reversible binding behaviour of Fe^{3+} with APQ.

Given the importance of logic gates in molecular keypad devices and molecular switches, reversibility experiment involving Fe^{3+} and EDTA were used as input signals for the same. Emission intensity at 140 a.u. was taken as the threshold value at wavelength 435 nm. A state OUT = 0 was given above the threshold value of the emission intensity, while a state OUT = 1 was given below it (Fig. 4).

In order to explore the practical applications of the developed fluorophore, quenching experiments were also performed by encapsulating APQ inside span80 (sorbitan ester of oleic acid) niosome. Niosomes are vesicular structures formed by self-assemblies of non-ionic surfactants. They mimic cell membranes in several aspects and potentially used as transdermal carriers for hydrophilic or hydrophobic drugs [40]. We have demonstrated confocal imaging (Fig. 5) in the span80 vesicular system by using the fluorescence of APQ with and without Fe^{3+}. Fig. 5a, b showed the bright field and the corresponding fluorescence images of vesicles loaded with APQ, when excited at 405 nm and emission was collected in the wavelength region of 460 ± 20 nm. As and when, APQ bound with Fe^{3+}, the fluorescence intensity was quenched significantly and very weak fluorescence was observed from the vesicles (Fig. 5d and f). These observations clearly indicated the interaction of APQ with Fe^{3+} inside the vesicle membrane, which can be suitably tailored for biological applications as required.

Experiments were also conducted to detect the iron concentration in water samples collected from different sources

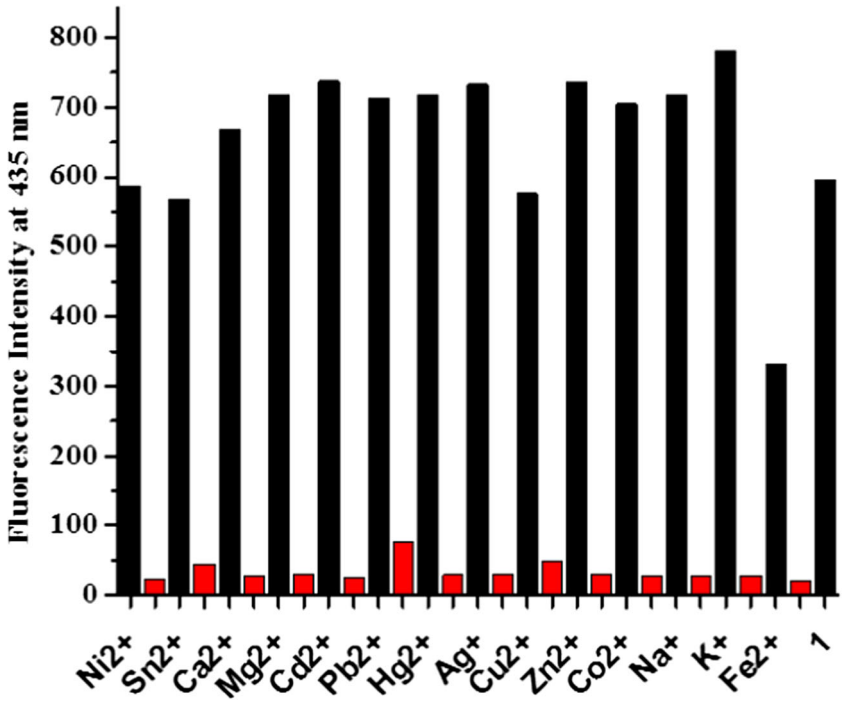

Fig. 2 Competitive selectivity (λ_{ex} = 320 nm and fluorescence was recorded at 435 nm) of APQ towards Fe^{3+} in DMF, in presence of other metal ions. **1**: only **APQ**. Black bar represents APQ + metal ions and red bar represents APQ + metal ions + Fe^{3+} ions

Fig. 3 Structure of ligands **3**, **4, 5** and **6**

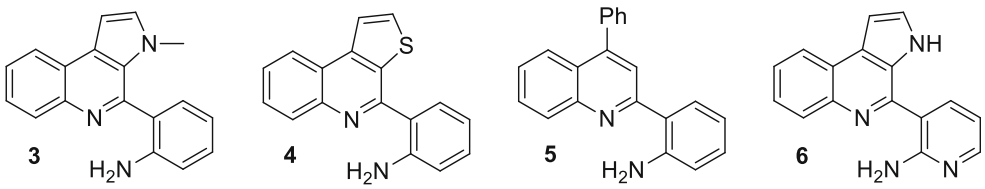

which further demonstrated the applicability of the developed sensor (ESI).

Conclusion

In summary, we have developed a sensor for selective micromolar detection of Fe^{3+}. The probe works by blocking the ESIPT reaction of the ligand in the presence of Fe^{3+} and performs optimally even in the presence of well-known interfering cations Co^{2+} and Cu^{2+}. Binding stoichiometry was found to be 2:1 for metal and ligand. The capability of the developed sensor was further demonstrated by its encapsulation inside vesicle membrane and detection of Fe^{3+} ions thereby.

Experimental

All the starting materials were purchased and used directly. Solvents were dried and distilled before use. Visualization on TLC was achieved by use of UV light (254 nm) or iodine. ^{1}H NMR (300 MHz and 400 MHz) and ^{13}C (75 MHz and 100 MHz) spectra were recorded in $CDCl_3$ and DMSO solution with TMS as internal standard. The mass spectrum was recorded on Agilent 1100/LC MSD Trap SL version. Column chromatography was performed on silica gel (100–200 mesh, SRL. India). Fluorescence studies were done on Hitachi F-7000 spectrofluorimeter.

Synthesis of 2-(3H-Pyrrolo[2,3-c]Quinolin-4-yl)Aniline (APQ) Synthesis of the compound was carried out as per the procedure described in reference [31].

^{1}H NMR (300 MHz, DMSO-d_6): δ 6.13 (s, 2H), 6.77 (t, J = 7.4 Hz, 1H), 6.92 (d, J = 8.1 Hz, 1H), 7.22 (s, 2H), 7.58 (t, J = 6.6 Hz, 4H), 8.06–7.97 (m, 1H), 8.36–8.25 (m, 1H), 11.69 (s, 1H). ^{13}C NMR (101 MHz, DMSO-d_6): δ 101.61 (s), 116.72 (s), 120.64 (s), 123.11 (s), 148.00 (s), 123.46 (s), 125.87 (s), 126.22 (s), 127.29 (s), 128.61 (s), 129.09 (s), 129.50 (s), 130.23, 141.74 (s), 147.56 (s).

Synthesis of 2-(3H-Pyrrolo[2,3-c]Quinolin-4-yl)Phenol (HPQ) Synthesis of the compound was carried out as per the procedure described in reference [31]. Structure confirmed by IR, ^{1}H, ^{13}C NMR and mass spectrum and was consistent with those described in the literature [31].

Synthesis of 2-(3-Methyl-3H-Pyrrolo[2,3-c]Quinolin-4-yl)Aniline (3) Synthesis of the compound was carried out as per the procedure described in reference [31].

^{1}H NMR (300 MHz, DMSO-d_6): δ 3.37 (s, 3H), 4.82 (s, 2H), 6.72 (t, J = 7.2 Hz, 1H), 6.85 (d, J = 8.0 Hz, 1H), 7.12 (d,

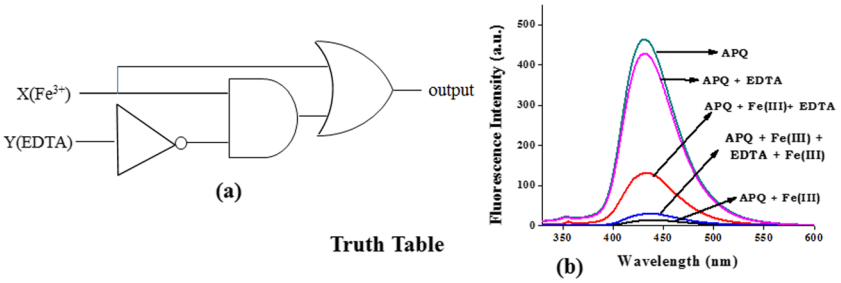

Truth Table

X (Fe^{3+})	Y(EDTA)	Out (Emission intensity at 435 nm)
0	0	0
0	1	0
1	0	1
1	1	1

(c)

Fig. 4 **a** $Fe^{3+}$and EDTA as chemical inputs and their effect on the emission spectra of APQ. **b** Emission spectra of APQ, EDTA and Fe^{3+}titrations. **c** Truth table incorporating logic functions

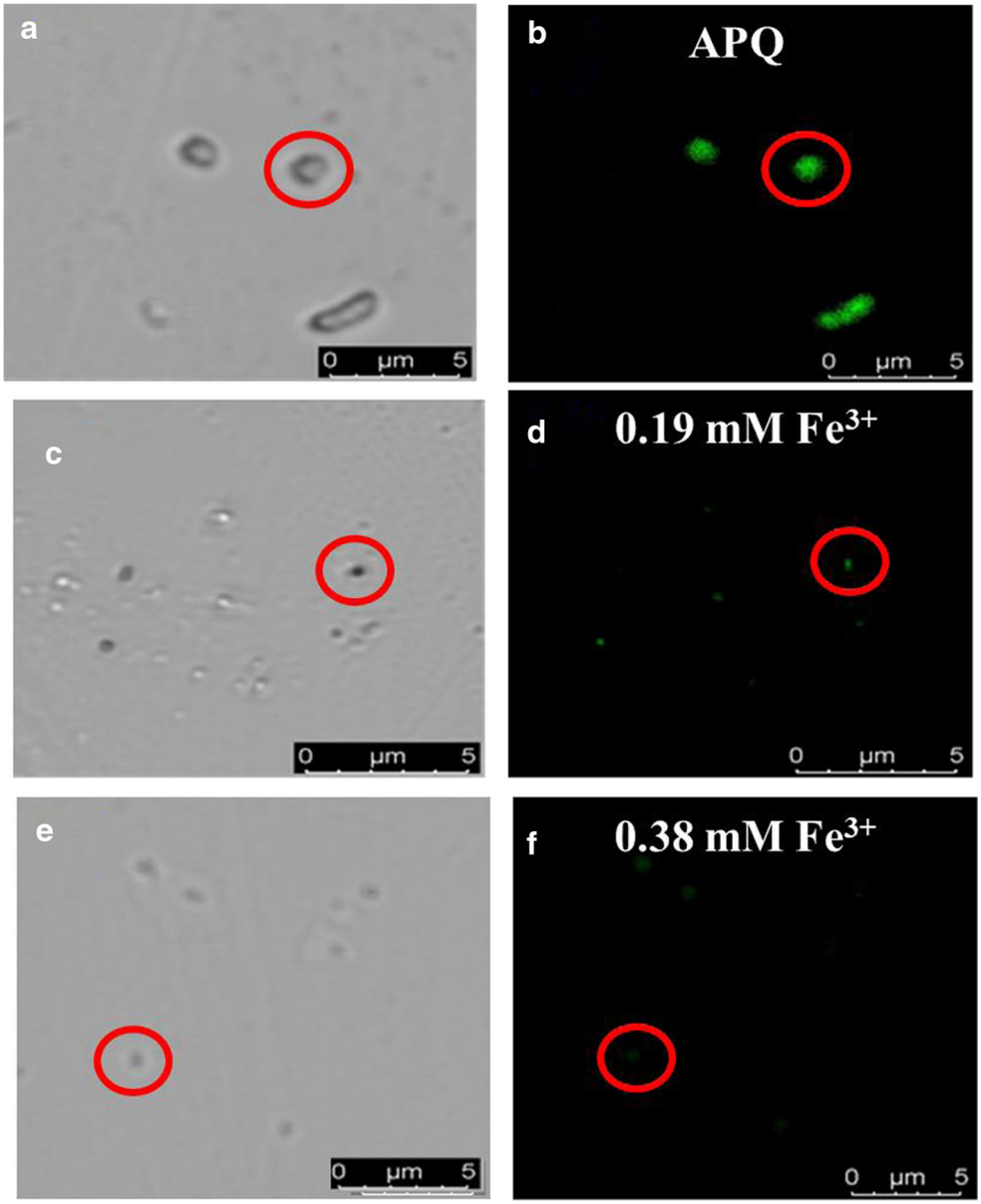

Fig. 5 Bright field (**a**, **c**, **e**) and fluorescence (**b**, **d**, **f**) Confocal images of span-80 niosomes loaded with APQ, with and without Fe^{3+}

J = 7.4 Hz, 1H), 7.20 (dd, J = 15.0, 5.1 Hz, 2H), 7.57 (dd, J = 6.1, 3.3 Hz, 3H), 8.00 (dd, J = 6.1, 3.4 Hz, 1H), 8.32 (dd, J = 6.2, 3.2 Hz, 1H). ^{13}C NMR (75 MHz, DMSO-d_6): δ 35.23 (s), 99.81 (s), 114.99 (s), 115.88 (s), 122.93 (d, J = 12.8 Hz), 125.59 (d, J = 10.0 Hz), 127.96 (s), 128.96 (s), 129.38 (s), 129.71 (s), 130.16 (s), 133.23 (s), 141.76 (s), 146.39 (d, J = 8.0 Hz).

Synthesis of 2-(Thieno[2,3-c]Quinolin-4-yl)Aniline (4) Synthesis of the compound was carried out as per the procedure described in reference [34].

^{1}H NMR (400 MHz, DMSO-d_6): δ 7.83–7.74 (m, 2H), 7.86 (ddd, J = 8.1, 7.4, 1.6 Hz, 1H), 7.96 (td, J = 7.5, 1.2 Hz, 1H), 8.01 (dd, J = 7.6, 1.4 Hz, 1H), 8.12–8.07 (m, 1H), 8.24 (dd, J = 8.1, 0.9 Hz, 1H), 8.34 (d, J = 5.3 Hz, 1H), 8.44 (d, J = 5.4 Hz, 1H), 8.64–8.60 (m, 1H). ^{13}C NMR (101 MHz, DMSO-d_6): δ 116.2, 116.8, 121.9, 123.2, 124.2, 127.1, 128.9, 129.3, 129.5, 130.8, 132.7, 134.1, 143.4, 144.1, 147.8, 154.2.

Synthesis of 2-(4-Phenylquinolin-2-yl)Aniline (5) Synthesis of the compound was carried out as per the procedure described in reference [35].

^{1}H NMR (400 MHz, DMSO-d_6): δ 6.68–6.62 (m, 1H), 6.87 (dd, J = 8.2, 1.1 Hz, 1H), 7.20–7.12 (m, 3H), 7.66–7.53 (m, 6H), 7.79 (ddd, J = 8.3, 6.9, 1.4 Hz, 1H), 7.84 (ddd, J = 8.3, 4.2, 1.0 Hz, 2H), 7.88 (s, 1H), 8.12 (d, J = 8.4 Hz, 1H). ^{13}C NMR (100 MHz, DMSO-d_6): δ 115.7, 116.6, 119.1, 120.0, 124.0, 125.0, 126.4, 128.5, 128.7, 128.9, 129.5, 129.7, 130.2, 137.5, 146.7, 148.1, 148.6, 158.4.

Synthesis of 3-(3H-Pyrrolo[2,3-c]Quinolin-4-yl)Pyridin-2-Amine (6) Synthesis of the compound was carried out as per the procedure described in reference [31].

^{1}H NMR (400 MHz, DMSO-d_6): δ 6.81 (dd, J = 7.4, 4.9 Hz, 1H), 6.91 (s, 2H), 7.27–7.23 (m, 1H), 7.66–7.57 (m, 3H), 8.01 (ddd, J = 9.2, 7.3, 2.8 Hz, 2H), 8.13 (dd, J = 4.9, 1.7 Hz, 1H), 8.33 (dd, J = 6.5, 3.0 Hz, 1H), 11.86 (s, 1H). ^{13}C NMR (101 MHz, DMSO-d_6): δ 101.78 (s), 113.02 (s), 115.31 (s), 123.22 (s), 123.50 (s), 126.19 (s), 126.40 (s), 127.24 (s), 128.90 (s), 129.13 (s), 129.71 (s), 138.25 (s), 141.57 (s), 145.82 (s), 148.98 (s).

Encapsulation of APQ in the Vesicle and Confocal Imaging

Niosomes were prepared using standard thin layer evaporation method [36]. Span80 surfactant and cholesterol were taken in the ratio 1:1. Afterward, this was dissolved in 2:1 chloroform/methanol mixture. These solvents were evaporated in a rotary-evaporator at 100 rpm and under a vacuum of 20 Hg at 30 °C to form a thin film, which was further hydrated with water. The suspension was vortexed and sonicated to get the final niosomal suspension. The prepared niosomes were first loaded with 10 μM of APQ. For quenching experiments, APQ loaded niosomes were further treated with 0.19 and 0.38 mM Fe^{3+} solutions. The niosomes were incubated with the formulation for 60 min and then imaged using a TCS SP8 spectral laser scanning confocal microscope.

Acknowledgements T.U.K. thanks CSIR and BITS-Pilani for PhD fellowship. S.V.P. thanks DST- inspire (IF150605) scheme for providing senior research fellowship. A.N. thanks DST-SERB (SB/FT/CS-129/2013) for financial support. A.B. thanks Council for Scientific and Industrial Research, New Delhi for research grant. Authors gratefully acknowledge support from Department of Science and Technology, India for the FIST grant SR/FST/CSI-240/2012.

References

1. Fernandez-Real JM, McClain D, Manco M (2015) Mechanisms linking glucose homeostasis and iron metabolism toward the onset and progression of Type 2 diabetes. Diabetes Care 38:2169–2176
2. Rathnasamy G, Ling E-A, Kaur C (2013) Consequences of iron accumulation in microglia and its implications in neuropathological conditions. CNS Neurol Disord Drug Targets 12:785–798
3. Lushchak V, Semchyshyn H (eds) (2012) Oxidative stress: molecular mechanisms and biological effects. Intech. https://doi.org/10.5772/2333
4. Youdim MBH (2008) Brain iron deficiency and excess; cognitive impairment and neurodegenration with involvement of striatum and hippocampus. Neurotox Res 14:45–56
5. Ohashi A, Ito H, Kanai C, Imura H, Ohashi K (2005) Cloud point extraction of iron(III) and vanadium(V) using 8-quinolinol derivatives and Triton X-100 and determination of 10moldm level iron(III) in riverine water reference by a graphite furnace atomic absorption spectroscopy. Talanta 65:525–530
6. Lunvongsa S, Oshima M, Motomizu S (2006) Determination of total and dissolved amount of iron in water samples using catalytic spectrophotometric flow injection analysis. Talanta 68:969–973
7. Gomes DMC, Segundo MA, Lima JLFC, Rangel AOSS (2005) Spectrophotometric determination of iron and boron in soil extracts using a multi-syringe flow injection system. Talanta 66:703–711
8. Tesfaldet ZO, van Staden JF, Stefan RI (2004) Sequential injection spectrophotometric determination of iron as Fe(II) in multi-vitamin preparations using 1,10-phenanthroline as complexing agent*1. Talanta 64:1189–1195
9. Yokoi K, Van den Berg CMG (1992) The determination of iron in seawater using catalytic cathodic stripping voltammetry. Electroanalysis 4:65–69
10. Bobrowski A, Nowak K, Zarebski J (2005) Application of a bismuth film electrode to the voltammetric determination of trace iron using a Fe(III)–TEA–BrO3− catalytic system. Anal Bioanal Chem 382:1691–1697
11. Elrod VA, Johnson KS, Coale KH (1991) Determination of subnanomolar levels of iron(II) and total dissolved iron in seawater by flow injection and analysis with chemiluminescence detection. Anal Chem 63:893–898
12. Qin W, Zhang ZJ, Zhang CJ (1998) Chemiluminescence flow sensor with immobilized reagents for the determination of iron(III). Microchim Acta 129:97–101
13. Kimura M, Tsunenaga M, Takami S, Ohbayashi Y (2005) Development of Functional Imidazole Derivatives: A Potential Chemiluminescent Chemosensor. Bull Chem Soc Jpn 78:929–931
14. Kikkeri R, Traboulsi H, Humbert N, Gumienna-Kontecka E, Arad-Yellin R, Melman G, Elhabiri M, Albrecht-Gary AM, Shanzer A (2007) Toward Iron Sensors: Bioinspired Tripods Based on Fluorescent Phenol-oxazoline Coordination Sites. Inorg Chem 46:2485–2497
15. Sahoo SK, Sharma D, Bera RK, Crisponi G, Callan JF (2012) Iron(III) selective molecular and supramolecular fluorescent probes. Chem Soc Rev 41:7195–7227
16. Lan L, Niu Q, Guo Z, Liu H, Li T (2017) Highly sensitive and fast responsive "turn-on" fluorescent sensor for selectively sensing Fe 3+ and Hg 2+ in aqueous media based on an oligothiophene derivative and its application in real water samples. Sensors Actuators B Chem 244:500–508
17. Hua C, Zheng H, Zhang K, Xin M, Gao J, Li Y (2016) A novel turn off fluorescent sensor for Fe(III) and pH environment based on coumarin derivatives: the fluorescence characteristics and theoretical study. Tetrahedron 72:8365–8372
18. Zhao B, Liu T, Fang Y, Wang L, Song B, Deng Q (2016) A novel colorimetric chemosensor based on quinoline for the sequential detection of Fe3+ and PPi in aqueous solution. Tetrahedron Lett 58:1025–1029
19. Joshi S, Kumari S, Bhattacharjee R, Sarmah A, Sakhuja R, Pant DD (2015) Experimental and theoretical study: determination of dipole moment of synthesized coumarin–triazole derivatives and application as turn off fluorescence sensor: High sensitivity for iron(III) ions. Sensors Actuators B Chem 220:1266–1278
20. Sharma D, Kuba A, Thomas R, Kumar R, Choi H-J, Sahoo SK (2016) An aqueous friendly chemosensor derived from vitamin B6 cofactor for colorimetric sensing of Cu2+ and fluorescent turn-off sensing of Fe3+. Spectrochim Acta A 153:393–396
21. Maity S, Kundu A, Pramanik A (2015) Synthesis of biologically important, fluorescence active 5-hydroxy benzo[g]indoles through four-component domino condensations and their fluorescence "Turn-off" sensing of Fe(iii) ions. RSC Adv 5:52852–52865

22. Wang W, Wei J, Liu H, Liu Q, Gao Y (2017) A novel colorimetric chemosensor based on quinoline for the sequential detection of Fe3+ and PPi in aqueous solution. Tetrahedron Lett 58:1025–1029
23. Mukherjee S, Talukdar S (2016) A reversible pyrene-based turn-on luminescent chemosensor for selective detection of Fe3+ in aqueous environment with logic gate application. J Fluoresc 26:1021–1028
24. Ghosh K, Rathi S (2014) A novel probe for selective colorimetric sensing of Fe(ii) and Fe(iii) and specific fluorometric sensing of Fe(iii): DFT calculation and logic gate application. RSC Adv 4: 48516–48521
25. Goswami S, Aich K, Das AK, Manna A, Das S (2013) A naphthalimide–quinoline based probe for selective, fluorescence ratiometric sensing of trivalent ions. RSC Adv 3:2412
26. Sen S, Sarkar S, Chattopadhyay B, Moirangthem A, Basu A, Dhara K, Chattopadhyay P (2012) A ratiometric fluorescent chemosensor for iron: discrimination of Fe2+ and Fe3+ and living cell application. Analyst 137:3335–3342
27. Ghosh K, Tarafdar D (2015) Piperazine-based new sensor: selective ratiometric sensing of Fe3+, logic gate construction and cell imaging. Supramol Chem 27:224–232
28. Akula M, El-Khoury PJ, Nag A, Bhattacharya A (2014) Selective Zn2+ sensing using a modified bipyridine complex. RSC Adv 4:25605
29. Akula M, Thigulla Y, Nag A, Bhattacharya A (2015) Selective detection of fluoride using fused quinoline systems: effect of pyrrole. RSC Adv 5:57231–57234
30. Zhang XB, Cheng G, Zhang WJ, Shen GL, Yu RQ (2007) A fluorescent chemical sensor for Fe3+ based on blocking of intramolecular proton transfer of a quinazolinone derivative. Talanta 71:171–177
31. Wang P, Liu X, Fu J, Chang Y, Yang L, Xu K (2018) Synthesis and fluorescence spectral studies of novel quinolylbenzothiazole-based sensors for selective detection of Fe3+ion. Can J Chem 96:835–841
32. Xue K, Wang P, Dong W, Luo X, Cheng P, Xu K (2018) Fluorescence Sensors for Fe3+ Ion with High Selectivity and Sensitivity and Bioimaging in Living Cells. Chem Select 3:11081
33. Wang P, Fu J, Yao K, Chang Y, Xu K, Xu Y (2018) A novel quinoline-derived fluorescent "turn-on" probe for Cu2+ with highly selectivity and sensitivity and its application in cell imaging. Sensors Actuators B Chem 273:1070–1076
34. Chang Y, Fu J, Yao K, Li B, Xu K, Pang X (2019) Novel fluorescent probes for sequential detection of Cu2+ and citrate anion and application in living cell imaging. Dyes Pigments 161:331–340
35. Akula M, Padma Sridevi J, Yogeeswari P, Sriram D, Bhattacharya A (2014) New class of antitubercular compounds: synthesis and anti-tubercular activity of 4-substituted pyrrolo[2,3-c]quinolines. Monatsh Chem 145:811–819
36. Avirah RR, Jyothish K, Ramaiah D (2008) Infrared absorbing croconaine dyes: synthesis and metal ion binding properties. J Org Chem 73:274–279
37. Ding Y, Xie Y, Li X, Hill JP, Zhang W, Zhu W (2011) Selective and sensitive "turn-on" fluorescent Zn2+ sensors based on di- and tripyrrins with readily modulated emission wavelengths. Chem Commun 47:5431–5433
38. Akula M, Yogeeswari P, Sriram D, Jha M, Bhattacharya A (2016) Synthesis and anti-tubercular activity of fused thieno-/furo-quinoline compounds. RSC Adv 6:46073–46080
39. Tang J, Wang L, Mao D, Wang W, Zhang L, Wu S, Xie Y (2011) Ytterbium pentafluorobenzoate as a novel fluorous Lewis acid catalyst in the synthesis of 2,4-disubstituted quinolines. Tetrahedron 67:8465–8469
40. Damera DP, Venuganti VVK, Nag A (2018) Deciphering the Role of Bilayer of a Niosome towards Controlling the Entrapment and Release of Dyes. Chem Select 3:3930